Early Phase Contingency Trajectory Design for the Failure of the First Lunar Orbit Insertion Maneuver: Direct Recovery Options

Young-Joo Song[†], Jonghee Bae, Young-Rok Kim, Bang-Yeop Kim
Korea Aerospace Research Institute, Daejeon 34133, Korea

To ensure the successful launch of the Korea pathfinder lunar orbiter (KPLO) mission, the Korea Aerospace Research Institute (KARI) is now performing extensive trajectory design and analysis studies. From the trajectory design perspective, it is crucial to prepare contingency trajectory options for the failure of the first lunar brake or the failure of the first lunar orbit insertion (LOI) maneuver. As part of the early phase trajectory design and analysis activities, the required time of flight (TOF) and associated delta-V magnitudes for each recovery maneuver (RM) to recover the KPLO mission trajectory are analyzed. There are two typical trajectory recovery options, direct recovery and low energy recovery. The current work is focused on the direct recovery option. Results indicate that a quicker execution of the first RM after the failure of the first LOI plays a significant role in saving the magnitudes of the RMs. Under the conditions of the extremely tight delta-V budget that is currently allocated for the KPLO mission, it is found that the recovery of the KPLO without altering the originally planned mission orbit (a 100 km circular orbit) cannot be achieved via direct recovery options. However, feasible recovery options are suggested within the boundaries of the currently planned delta-V budget. By changing the shape and orientation of the recovered final mission orbit, it is expected that the KPLO mission may partially pursue its scientific mission after successful recovery, though it will be limited.

Keywords: contingency trajectory design, lunar orbit insertion failure, direct recovery, Korea pathfinder lunar orbiter

1. INTRODUCTION

The Korea pathfinder lunar orbiter (KPLO), an experimental lunar orbiter that will orbit the Moon, is scheduled for launch in late 2020 through an international collaboration. For the nominal mission operation of the KPLO, an altitude of approximately 100±30 km will be maintained around the Moon, with a mission duration of no longer than 12 months, including the commissioning phase. The launch mass of the KPLO is expected to be approximately 550 kg, including the scientific payload mass of approximately 40 kg (Song et al. 2016b). For the KPLO mission, a total of six instruments (five from Korea and one from National Aeronautics and Space Administration (NASA)) will be installed on board to complete the primary mission objectives, including verification of disruption tolerant network (DTN) methodologies. The KPLO instruments and developers include the lunar terrain imager (LUTI) by the Korea

Aerospace Research Institute (KARI), polarimetric camera (PolCam) by the Korea Astronomy and Space Science Institute (KASI), KPLO gamma ray spectrometer (KGRS) by the Korea Institute of Geoscience and Mineral Resources (KIGAM), KPLO magnetometer (KMAG) by KyungHee University (KHU), and the shadow camera (ShadowCam) by investigators at Arizona State University (ASU) and Malin Space Science Systems (MSSS) as a NASA contribution. Additionally, the Electronics and Telecommunications Research Institute (ETRI) of Korea and NASA are working together to develop and demonstrate DTN technologies (Song et al. 2017).

To ensure the successful launch of the KPLO, KARI is now performing extensive trajectory design and analysis activities, including joint efforts between KARI and NASA to validate the trajectory design and navigation performance. Several preliminary design studies have already been conducted for lunar mission trajectory design and analysis (Song et al.

2008; Song et al. 2009; Song et al. 2010; Woo et al. 2010; Song et al. 2011; Choi et al. 2013; Song & Kim 2015) as well as orbit determination analysis (Kim et al. 2017; Lee et al. 2017). However, most of the previous work was mainly focused on the optimal trajectory generation from the nominal trajectory planning point of view. With the necessity of obtaining uncertainty requirements regarding orbit, attitude, and burn performance for the critical maneuvers, Bae et al. (2016) and Song et al. (2016a) performed dispersion analyses on the first lunar orbit insertion (LOI) and mid-course correction (MCC) maneuvers, respectively. Regardless of the many preliminary trajectory design and analysis activities conducted so far, it is crucial to plan contingency trajectory options to prepare for the malfunction of maneuver executions.

Establishing contingency trajectories and planning associated backup options are among the important activities during the mission design phase. These areas of study have always been the focus in past lunar missions, such as the lunar prospector (LP) (Lozier et al. 1998), lunar reconnaissance orbiter (LRO) (Bechman 2007; Houghton et al. 2007), selenological and engineering explorer (SELENE) (Kawakatsu et al. 2007), lunar atmosphere dust and environment explorer (LADEE) (Genova 2014), and Chang'e-3 (CE-3) (Liu et al. 2015) missions. Among the numerous maneuvers to be executed during the entire lunar mission phase, preparing contingency trajectory options for the first LOI maneuver failure is very critical, as the successful execution of the first LOI maneuver directly leads to successful lunar capture. Malfunctions of relatively small maneuvers, such as MCCs, would have relatively small effects on the entire mission trajectory, as there would be another chance of correction by adding other small correction maneuvers. However, the malfunction of the first LOI may result in a lunar sphere of influence (SOI) escape within a short duration due to large velocity changes and the lunar swing-by effect. Generally, there are two typical trajectory recovery options for the first LOI maneuver execution failure - direct recovery and low energy recovery. Direct recovery options have many benefits, such as a simple trajectory, easy implementation, and short flight time. However, direct recovery options require quite large orbital energy to recover the mission trajectory (Liu et al. 2015). Low energy recovery options can save a remarkable amount of fuel, though they require very long flight times of more than several hundred days of return flight (Genova 2014; Liu et al. 2015).

Current work analyzed contingency trajectory options for the KPLO mission to prepare for the failure of the first LOI maneuver. The direct recovery option was considered first with regard to the current design life time of KPLO (about one year including the commissioning phase) and to focus on the early phase mission design and analysis activities. Preliminary analysis on the contingency trajectory design was performed

and the associated delta-Vs, as well as the trajectory characteristics, were obtained, including the required time of flight (TOF) between each recovery maneuver (RM) and the associated delta-V magnitudes to recover the KPLO mission trajectory. In addition, the possibility of two different mission orbit recovery cases, insertion into circular mission orbit or insertion into elliptical mission orbit, were proposed within the direct recovery options to find more feasible recovery solutions for the KPLO mission. In Section 2, the simulation method is described in detail, including the equations of motion with the strategy used to compute RMs for each different transfer leg. Simulation backgrounds are provided with detailed nominal lunar orbit acquisition (LOA) phase characteristics in Section 3. Simulation results are analyzed in Section 4 for both proposed mission orbit recovery cases: insertion into circular and elliptical mission orbits. Finally, concluding remarks are made in Section 5. Based on the current analysis results, more detailed contingency trajectory options or in depth analyses will be conducted for the KPLO mission, including low energy recovery cases to extend KPLO's contingency trajectory recovery options.

2. CONTINGENCY TRAJECTORY DESIGN METHOD

2.1 Equations of Motion

Two-body equations of motion of the spacecraft flying in the vicinity of the Moon can be expressed as (Vallado 2013):

$$\dot{\boldsymbol{r}} = \boldsymbol{v} \tag{1}$$

$$\dot{\boldsymbol{v}} = -\frac{\mu \boldsymbol{r}}{r^3} \tag{2}$$

where μ is the gravitational constant of the Moon, and $\boldsymbol{r}$ and $\boldsymbol{v}$ denote position and velocity vectors of the spacecraft, respectively. With the initial position ($\boldsymbol{r}_0 = \boldsymbol{r}_{hyp}$) and velocity ($\boldsymbol{v}_0 = \boldsymbol{v}_{hyp} + \Delta \boldsymbol{v}_{LOI}^{1st}$) vectors, the spacecraft will be captured successfully into the lunar orbit after the first LOI maneuver execution. The terms, $\boldsymbol{r}_{hyp}$ and $\boldsymbol{v}_{hyp}$, denote the hyperbolic arrival position and velocity vectors of the spacecraft at the moment of periapsis arrival. $\Delta \boldsymbol{v}_{LOI}^{1st}$ is the applied first LOI maneuver, assumed as an impulsive burn, to facilitate lunar capture of the spacecraft. If the first lunar brake or execution of $\Delta \boldsymbol{v}_{LOI}^{1st}$ fails due to various reasons during the real operation, then the spacecraft will fly away from the Moon requiring additional trajectory recovery plans. In the early system design and analysis phase, every necessary maneuver to recover trajectory is assumed to be an impulsive burn in further discussions.

2.2 Recovery Maneuver Computation

In case of the failure of the first LOI maneuver, the contingency trajectory design problem can be solved by the orbital boundary value problem, finding the trajectory connecting two given points with a flight time. Therefore, at least two additional RMs will be necessary to capture the spacecraft into an orbit around the Moon. Note that these assumptions are only valid within the direct recovery case. The RM #1 will be applied to adjust the trajectory toward the Moon, and the RM #2 will insert the spacecraft into an orbit around the Moon. To solve the orbital boundary value problem, the current work applied the widely known Lambert theory to compute the characteristics of the RMs. Since the first accurate solutions of the Lambert's problem by Gauss (1857), many authors have devoted their efforts to advancing solutions to Lambert's problem, including Lancaster & Blanchard (1969), Bate et al. (1971), Gooding (1990), Battin (1999). Among these methods, Gooding's method was found to be the most stable method when considering numerical stability as well as computational complexity (Izzo 2015). Therefore, the current work adapted the given contingency trajectory design problem into the widely known Lambert theory and solved it with Gooding's method. To solve Lambert's problem via Gooding's solution, the current work derived both the position and velocity vectors at the moment of the RM #1 execution (r_{RM1}, v_{RM1}) and RM #2 execution (r_{RM2}, v_{RM2}).

To compute r_{RM1} and v_{RM1}, r_{hyp} and v_{hyp} are obtained from r_0 and v_0 with the assumption that $r_{hyp} = r_0$ is still valid, as the current work assumed every maneuver to be an impulsive burn. Therefore, v_{hyp} can simply be computed by:

$$v_{hyp} = M^{-1} \begin{bmatrix} v_r \hat{u}_r \\ v_t \hat{u}_t \\ v_n \hat{u}_n \end{bmatrix} \tag{3}$$

where M is the state transition matrix that converts states expressed in the inertial frame into the radial-tangential-normal (RTN) frame with unit vector components of $\hat{u}_r$, $\hat{u}_t$, and $\hat{u}_n$. In addition, v_r, v_t, and v_n are the periapsis velocity vector components of the approach hyperbolic trajectory, where subscripts r, t and n indicate the radial, tangential, and normal direction of each component. The periapsis velocity vector components may be defined as $v_t = v_{app}$ and v_r, $v_n = 0$ where v_{app} is the magnitude of the hyperbolic approach velocity at periapsis. M can be computed using r_0 and v_0, and these vectors can be obtained directly using the first capture orbit's six orbital elements (a_0, e_0, i_0, ω_0, Ω_0, v_0), which are all pre-designed parameters. The semi-major

axis, a_0, of the first capture orbit can be computed using the desired orbital period of the first capture orbit, P; and eccentricity, e_0, can be derived using the mission dependent radius of the closest approaching periapsis, r_p, as shown in Eq. (4) (Brown 1998).

$$a_0 = \left(\frac{(P/2\pi)^2}{\mu} \right)^{\frac{1}{3}} \tag{4a}$$

$$e_0 = 1 - \frac{r_p}{a_0} = 1 - \frac{R_m + h_p}{a_0} \tag{4b}$$

In Eq. (4), R_m is the mean radius of the Moon, and h_p is the periapsis altitude at the moment of the closest lunar approach, which is also a pre-defined value. Other elements, such as the inclination, i_0, argument of periapsis, ω_0, right ascension of ascending node, Ω_0, and true anomaly, v_0, are mission dependent parameters determined during mission definition or the LOA phase design. After successful derivation of r_{hyp} and v_{hyp}, those states are numerically propagated during t_{RM1} to find r_{RM1} and v_{RM1}, where t_{RM1} is the elapsed time since the first LOI execution time that is nominally planned. Hereinafter, t_{RM1} is termed TOF Leg 1. For r_{RM2} and v_{RM2} computation, the final orbital elements (a_f, e_f, i_f, ω_f, Ω_f, v_f) of the spacecraft, again pre-targeted values for the successful trajectory recovery options, are used directly.

With given values for r_{RM1}, v_{RM1}, r_{RM2}, v_{RM2}, μ, and t_{RM2}, the established contingency trajectory design problem can be solved by Gooding's method, where t_{RM2} indicates the elapsed time between the execution of RM #1 and RM #2 execution at r_{RM2} and is defined as TOF Leg 2 in the following discussions. After solving Lambert's problem using Gooding's method, the initial, v_{RM1}^{Tras}, and final, v_{RM2}^{Tras}, velocity vectors of the recovery trajectory can be obtained and, with simple mathematics, the required velocity changes for both RMs, Δv_{RM1} and Δv_{RM2}, can be determined. For more details on Gooding's solution procedure for Lambert's problem, i.e., the kinematic geometry, iteration process, flight-time, and velocity computation algorithms, including the FORTRAN subroutine code, readers may refer to the work done by Gooding (1990). In Fig. 1, the corresponding geometry of the RM executions is depicted.

3. SIMULATION BACKGROUNDS

3.1 Assumptions and Setups

As previously discussed, the current study focused on establishing a contingency trajectory design strategy for the early mission design phase; therefore, two-body equations
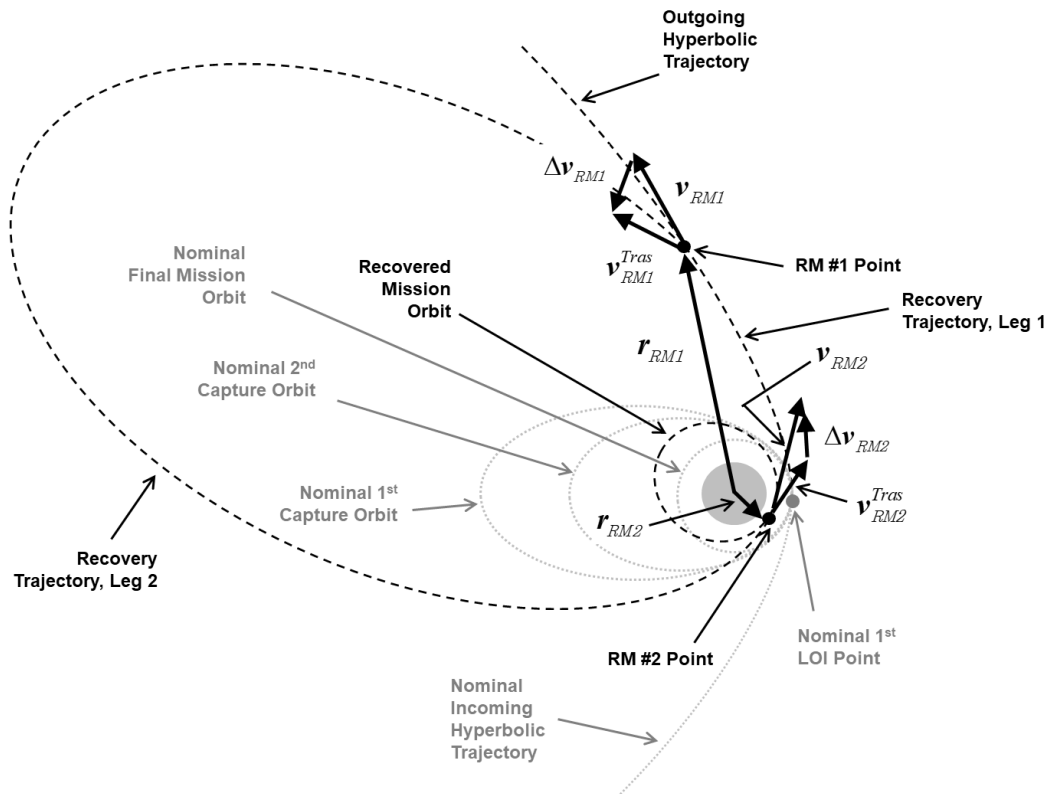
Fig. 1. Geometry of recovery maneuver execution (not to scale).

of motion were used, and every necessary burn to recover trajectory was assumed to be an impulsive maneuver. To integrate the equations of motion, the numerical integrator function of "ODE113" provided by MATLAB® is used. During the solution of Lambert's problem via Gooding's method, the following additional constraints are considered. The lower and upper boundary conditions are given as 1 to 24 hours for t_{RM1} and 1 to 30 days for t_{RM2}, and those durations are equally divided into 100 steps to search for the best solutions to minimize the overall RM magnitudes defined as $\left|\Delta v_{RMs}\right| = \left|\Delta v_{RM1}\right| + \left|\Delta v_{RM2}\right|$. These conditions indicate that RM #1 is executed within at least 1 to 24 hours after the nominal first LOI burn failure, and RM #2 is executed within 1 to 30 days after the execution of RM #1. The sum of t_{RM1} and t_{RM2} can be regarded as the total flight time, Δt_{TOF}, required to recover the trajectory. The selected boundaries are given from numerous trials during the simulations. Among the recovery trajectory solutions obtained, those solutions having spacecraft-Moon distances more than 64,000 km, the lunar sphere of influence distance, are automatically rejected to focus on two-body dynamics. To compute r_{hyp} and v_{hyp}, the following conditions are used. For r_{hyp} computation, r_0 is computed by using the pre-defined first nominal capture orbit conditions: $i_0 = 90°$ with ω_0, Ω_0, and v_0 set to 0°. The other orbital elements, a_0 and

e_0, are determined from the pre-defined v_{app}, P, and h_p. P is assumed to be 12 hours, and h_p is given as 100 km in altitude above the lunar surface. For v_{hyp} derivation, v_{app} is assumed to be about 2.497 km/s, which is the current estimate of the hyperbolic velocity magnitude at periapsis approach for nominal KPLO trajectory design results. The current study proposed the possibilities of two different recovery cases, insertion into circular mission orbit (hereinafter Case 1) and insertion into elliptical mission orbit (hereinafter Case 2), within the direct recovery options. The two recovery cases differ from each other by the shape of the mission orbit after recovery. The Case 1 recovered mission orbit has a circular shape with h_p of 30, 50, 100, 200, 500, and 1,000 km. Case 2 has a slight modification of the recovered mission orbit's shape with elliptical orbits having h_p of 30, 50, and 100 km. The current work analyzed Case 2 to investigate feasible recovery options that can be achieved within the boundaries of the current fuel budgets for the KPLO mission while partially performing its scientific mission after recovery. To compute v_{RM2} for each case, a circular orbit with $i_f = 90°$ and ω_f, Ω_f, and v_f set to 0° is used for Case 1 with the derivation of P consistent with given altitudes of h_p. For Case 2, shape as well as the orientation of the recovered mission orbit is changed to an elliptical orbit with $\omega_f = 45°$, with other orbital elements the same as in Case 1 except for a_f

Table 1. Summary of the orbital characteristics for the two orbit recovery cases

Recovered orbit's characteristics	Recovery Option Case 1	Recovery Option Case 2
Orbital shape	Circular mission orbit	Elliptical mission orbit
Considered periapsis altitude (km)	30, 50, 100, 200, 500, and 1,000	30, 50, and 100
Semi-major axis	Computed using periapsis altitude	Computed using available RM2 magnitude with consideration of periapsis altitude
Eccentricity	0	↑
Inclination (°)	90	←
Right Ascension of Ascending Node (°)	0	←
Argument of Periapsis (°)	0	45 (re-oriented)
True Anomaly (°)	0	←

Table 2. Expected event sequences and associated values for the nominal LOA phase

No.	Sequence Title	Parameters	Values (Units)	Remark
1	Hyperbolic arrival for 1st burn	Periapsis arrival velocity	2.497 (km/s)	Required velocity at the 1st capture orbit periapsis: 2.132 km/s
2	LOI #1	Delta-V magnitude	364.980 (m/s)	Insert spacecraft into the 1st capture orbit
3	Periapsis approach for 2nd burn	Periapsis approach velocity	2.132 (km/s)	Required velocity at the 2nd capture orbit periapsis: 1.881 km/s
4	LOI #2	Delta-V magnitude	250.534 (m/s)	Insert spacecraft into the 2nd capture orbit
5	Periapsis approach for 3rd burn	Periapsis approach velocity	1.881 (km/s)	Required velocity for "100 km" circular orbit: 1.634 km/s
6	LOI #3	Delta-V magnitude	247.550 (m/s)	Insert spacecraft into the final mission orbit

and e_f. a_f and e_f are derived according to the possible delta-V margins allocated to the KPLO mission with the assumed h_p values for Case 2. By properly changing ω_f for the recovered mission orbit, it is expected that KPLO may partially pursue its scientific mission after a successful recovery, though it will be limited. In Table 1, the characteristics of the two recovery cases are summarized.

3.2 Nominal Lunar Orbit Acquisition Phase

Before discussing the recovery options obtained from the current work, the nominally planned capture sequence for the KPLO mission, including the delta-Vs magnitudes for each LOI burn, is briefly summarized. This is intended to give the background for the nominal capture sequence currently planned for the KPLO mission and to provide insights into the following analysis of the results. During the LOA phase, the KPLO will be inserted into its final mission orbit by establishing a two phasing loop orbit around the Moon after the arrival of the periapsis by a hyperbolic approach. The first and second capture orbits will have orbital periods of about 12 hours and about 3.5 hours, respectively, and the KPLO will be placed into its mission orbit, a polar circular orbit at an altitude of 100 km with an orbital period of about 118 min. The current estimate of nominal periapsis hyperbolic approach velocity, v_{app}, is found to be about 2.497 km/s. It is assumed that two-body equations of motion are used

and every phasing orbit's periapsis altitude as well as the altitude of the mission orbits (100 km) are the same. This allows the periapsis velocity for each phasing loop orbit as well as the circular velocity of the final mission orbit to be derived by using pre-defined periods for each orbit. As v_{app} is already known, the required delta-Vs for each LOI burn can be easily determined. The expected event sequences for the LOA phase are summarized in Table 2; however, note that the sequence and associated values are only valid for the early stage mission design and analysis phase and may differ from sophisticated trajectory design results using N-body dynamics with finite burn maneuver models. As shown in Table 2, the sum of all LOI magnitudes, the expected overall delta-Vs for the LOA phase, is found to be approximately 863.064 m/s. Note that this 863.064 m/s of delta-V is an ideal value that is required only for the LOA phase except for the delta-V required for the trans lunar injection (TLI) burn. In addition to the ideal delta-Vs for the LOA phase, maximum delta-Vs of about 200 m/s are additionally allocated for the total delta-V budget for the KPLO mission, including launch window extension, launcher dispersions, mid-course correction maneuvers (MCC), system margins, etc. Overall delta-Vs of about 1.063 km/s can further be utilized for recovering the trajectory, even if the original mission life time may be shortened. Fig. 2 shows the nominally planned capture and mission orbits for the LOA phase.
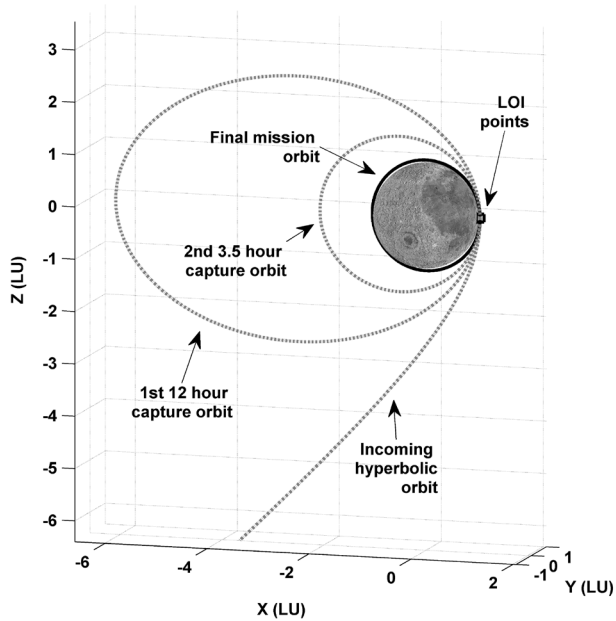
Fig. 2. Nominally planned LOA phase orbit (1 lunar unit (LU) = 1,738.2 km).

4. RECOVERY OPTION ANALYSIS

4.1 Case 1 - Insertion into Circular Mission Orbit

As already discussed, Case 1 assumes that the recovered mission orbit is a circular orbit with different h_p of 30, 50, 100, 200, 500, and 1,000 km. To search for the best execution time for RM #1 and RM #2 that minimize the magnitudes of the RMs (the best TOF Leg 1 and TOF Leg 2). As a result, a quicker execution of the first RM after the failure of the first LOI plays a significant role in reducing the overall magnitudes of the RMs. However, it is concluded that the TOF Leg 1 should be within the boundaries of 4.0 to 6.0 hours and the TOF Leg 2 from 5.0 to 5.5 days regardless of the recovered circular orbit's altitude. To arrive at these conclusions, system engineering and ground operation aspects, such as the considerable amount of time required for precise orbit determination, mission planning, and command generation validation, etc., are considered. In Fig. 3, the characteristics of the required RM magnitudes as a function of TOF Leg 1 and TOF Leg 2 for a 100 km circular orbit recovery case are shown. As shown in Fig. 3(a), it is clear that RM #1 should be executed as soon as possible if the first LOI burn is a failure. However, during the real operation, a considerable amount of time is necessary, at least several hours or more for RM #1 execution. This is to obtain knowledge of the spacecraft's exact orbital status as well as to plan and validate further recovery options. For TOF Leg 2, the magnitude of RM #2 is strongly influenced by the TOF Leg 1. For the same TOF Leg 1 conditions, spending
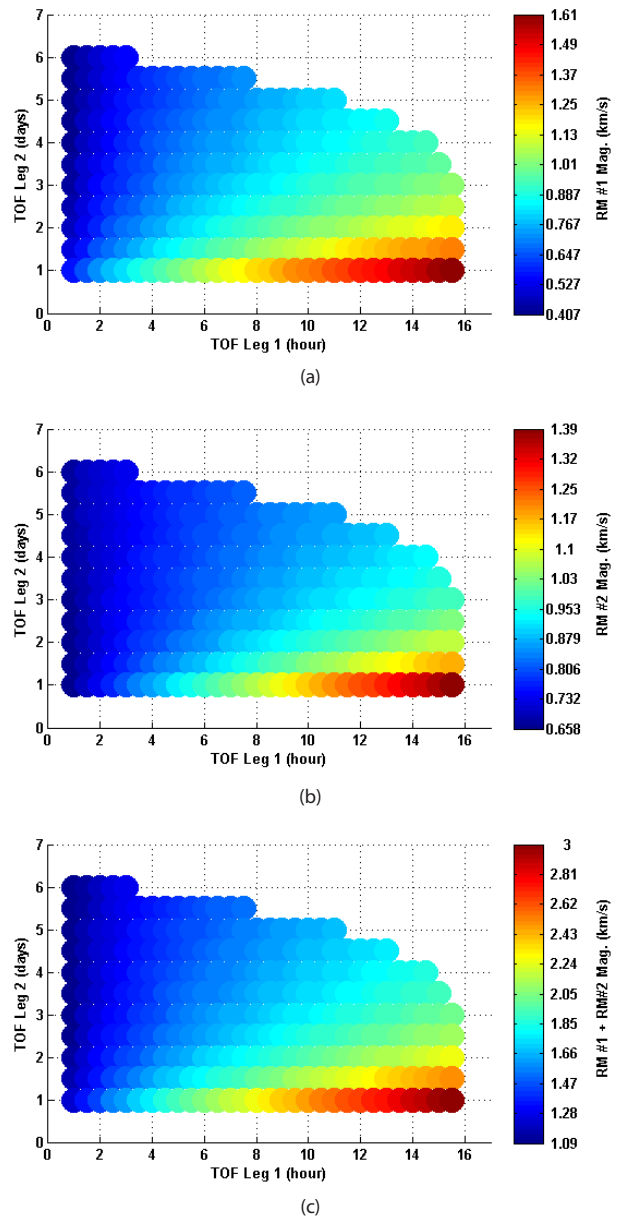

Fig. 3. Required RM magnitudes ((a) RM #1, (b) RM #2, and (c) overall RMs) as a function of TOF Leg 1 and TOF Leg 2 for a 100 km circular orbit recovery case.

more time for Leg 2 mostly requires less delta-Vs for RM #2 as shown in Fig. 3(b). The characteristics of the required overall delta-V magnitude for the RMs are depicted in Fig. 3(c).

A summary of the minimum and maximum RM magnitudes for different orbit altitudes is shown in Table 3 when TOF Leg 1 is selected to be from 4.0 to 6.0 hour and TOF Leg 2 from 5.0 to 5.5 days. As shown in Table 3, the required magnitude of RM #1 is increased with an incremental increase in the target altitude of the recovery orbit, though the increment is very small. Unlike the RM #1 magnitude tendency, the magnitude of RM #2 is greatly reduced with an incremental increase in the

Table 3. Minimum and Maximum RM magnitudes for different orbit altitudes when the TOF Leg 1 is from 4.0 to 6.0 hour and the TOF Leg 2 is from 5.0 to 5.5 days

Recovered circular orbit altitude (km)	RM #1 Mag. (km/s)		RM #2 Mag. (km/s)		RM #1 + RM #2 Mag. (km/s)	
	Min.	Max.	Min.	Max.	Min.	Max.
30	0.612	0.694	0.787	0.824	1.398	1.519
50	0.612	0.695	0.779	0.817	1.392	1.513
100	0.613	0.695	0.764	0.802	1.377	1.498
200	0.615	0.697	0.734	0.773	1.350	1.470
500	0.621	0.701	0.660	0.699	1.181	1.400
1,000	0.625	0.708	0.565	0.603	1.190	1.312
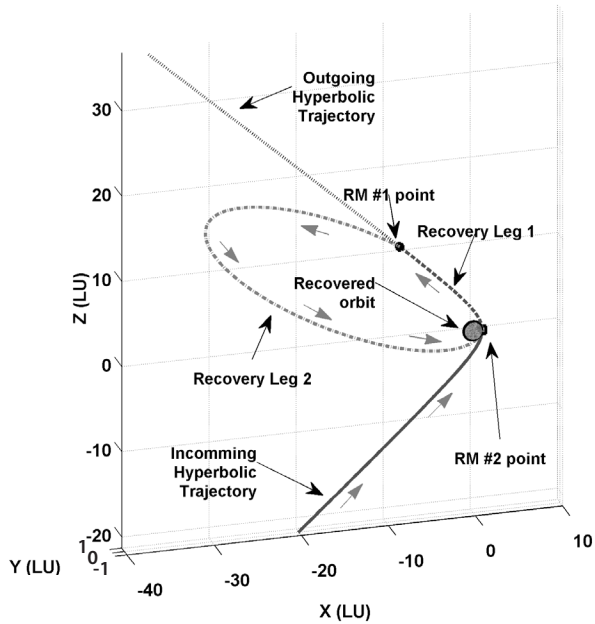
Fig. 4. Example recovery trajectory. Direct insertion into a 100 km by 100 km circular polar orbit case. TOF Leg 1 and Leg 2 are selected to be 4.0 hour and 5.0 day, respectively.

recovery orbit's target altitude. The RM #2 magnitude decrease can be understood by the fact that the approach velocity of the spacecraft at the moment of the RM #2 execution point gets smaller with the incremental increase in target altitude. Although the required overall magnitude of the RMs decreased with an incremental increase in the target altitude of the recovered circular orbit, the required overall RM magnitude to recover the mission orbit still exceeds the overall delta-V budget allocated for the KPLO mission including margins of about 1.063 km/s. Therefore, it can be concluded that the recovery strategy shown here can never be achieved under the delta-V budget currently allocated for the KPLO system design. In Fig. 4, an example recovery trajectory is shown for the case of direct insertion into a 100 by 100 km circular polar orbit. To plot this example, TOF Leg 1 and Leg 2 are selected to be 4.0 hour and 5.0 day, respectively, and the required overall RM magnitude is found to be about 1.377 km/s.

4.2 Case 2 - Insertion into Elliptical Mission Orbit

In the previous section, it is concluded that the Case 1 recovery option is not achievable within the currently allocated delta-V budget for the KPLO system design. Therefore, this sub-section discusses recovery options that can be possible within the delta-V budget currently allocated. A slightly different approach is used during the simulation to enforce the overall magnitude of the RMs used during the recovery. The overall magnitude of the RMs is intentionally adjusted to not exceed the value of the nominally planned overall magnitude of the delta-Vs (about 0.863 km/s) allocated for the KPLO LOA phase. Both RM #1 and RM #2 are derived by solving the Lambert problem as in Case 1, and the magnitude of RM #2 is replaced with a value that is recalculated using nominally planned and derived RM #1 magnitudes. By applying this strategy, the shape of the recovered orbit will no longer be circular but will be elliptical. With this approach, candidates for recovered mission orbits that can be achieved within the allocated delta-V budget can be investigated. As a result, the achievable orbital shapes using this approach are summarized in Table 4 with respect to different periapsis orbit altitudes after successful recovery. For this simulation, TOF Leg 1 is bounded within 4 ~ 6 hours and TOF Leg 2 within 5 ~ 6 days. Note that the values shown in Table 4 are the averages of all the candidates obtained.

As shown in Table 4, regardless of the periapsis altitude of the recovered mission orbit, it is found that about 0.655 km/s of RM #1 is required to adjust the trajectory toward the Moon. Therefore, slightly more or less than 0.200 km/s of velocity change can be allocated for the RM #2 execution. With about 0.200 km/s for RM #2, the achieved shape of the final recovered mission orbit is too elliptical to perform the scientific mission of the KPLO mission originally planned. For example, the orbital altitude at the moment of north- and south-pole approach is found to be about 1,137.778 km when the periapsis altitude is targeted to be 30 km. If the targeted periapsis is greater than 30 km, then the north- and south-pole approach altitude is also higher than 1,137.778 km. Note

Table 4. Achievable orbital shape after recovery with respect to different periapsis altitudes when the overall RM magnitude is limited to 0.863 km/s

	Periapsis altitudes						
	30	50	100	200	300	500	1,000
TOF Leg 1 (hour)	5.00	5.00	5.00	5.00	5.00	5.00	4.91
TOF Leg 2 (days)	5.25	5.25	5.25	5.25	5.25	5.25	5.32
RM #1 Mag. (km/s)	0.654	0.654	0.655	0.657	0.658	0.662	0.667
RM #2 Mag. (km/s)	0.209	0.209	0.208	0.206	0.205	0.201	0.196
Semi major axis (km)	4,574.738	4,603.837	4,676.338	4,820.391	4,963.383	5,247.026	5,867.997
Eccentricity	0.60938	0.60747	0.60278	0.59376	0.58517	0.56924	0.52857
Period (hour)	7.743	7.817	8.002	8.374	8.749	9.508	11.248
Apoapsis altitude (km)	5,643.477	5,681.675	5,776.676	5,964.782	6,150.766	6,518.052	7,259.995

Table 5. Expected orbital shape of recovered orbit with periapsis altitude of 30 km

Parameters	Delta-V margin applied to RM #2 (m/s)		
	0	100	200
RM #2 Mag. (km/s)	0.208	0.308	0.408
Semi major axis (km)	4,590.443	3,302.130	2,608.488
Eccentricity	0.61064	0.46184	0.32024
Orbital period (hour)	7.783	4.738	3.324
Apoapsis altitude (km)	5,674.488	3,098.261	1,710.976
Altitude at north pole passage (km)	3,328.709	2,119.888	1,288.517
Altitude at south pole passage (km)	271.4732	219.5140	170.1137
Altitude at ascending Node passage (km)	272.4051	220.0940	170.5752
Altitude at descending Node passage (km)	3,323.912	2,118.365	1,287.837

*Magnitude of RM #1 is about 0.655 km/s for this case.

Table 6. Expected orbital shape of recovered orbit with periapsis altitude of 50 km

Parameters	Delta-V margin applied to RM #2 (m/s)		
	0	100	200
RM #2 Mag. (km/s)	0.208	0.308	0.408
Semi major axis (km)	4,619.227	3,323.067	2,625.240
Eccentricity	0.60872	0.45919	0.31695
Orbital period (hour)	7.857	4.784	3.356
Apoapsis altitude (km)	5,712.455	3,120.135	1,724.480
Altitude at north pole passage (km)	3,367.221	2,145.563	1,305.910
Altitude at south pole passage (km)	293.561	240.857	190.544
Altitude at ascending Node passage (km)	294.491	241.417	190.975
Altitude at descending Node passage (km)	3,362.506	2,144.041	1,305.238

*Magnitude of RM #1 is about 0.655 km/s for this case.

that the current work is performed under the condition that the spacecraft's closest approach point to the Moon from recovery Leg 2 is located near the lunar equator, indicating that the location of the RM #2 execution as well as the periapsis of recovered orbit is near the lunar equator. With a highly elliptical recovered mission orbit having periapsis located near the lunar equator, most of the nominally planned scientific mission of the KPLO cannot be performed with the associated payloads, as their design basis indicates operation at 100±30 km or slightly more above the lunar surface. The operation ranges of the LUTI can be very limited to the flight times when altitudes are near the 100 km range. For the ShadowCam operation, results would be almost meaningless when flight altitudes of the near polar-regions are more than 1,000 km.

One of the alternative solutions for maximizing the scientific information obtained in the contingency situation is the adjustment of the recovered orbital shape to match the originally planned flight requirements insofar as possible. As an example, if the sub-spacecraft point at the periapsis passage (the RM #2 execution location) is adjusted and its altitude lowered, then the operation ranges of LUTI may expand even with the elliptical shape of the mission orbit. There could be some candidate elliptical mission orbits in which ShadowCam can be operated partially to either cover lunar south or north poles. In addition, such an orbit adjustment could benefit the quality of the KMAG measurements as the flight altitude is much lower than the altitudes nominally planned. In Tables 5-7, the expected orbital shape of the recovered orbit is summarized. To derive the results shown in Tables 5-7, the periapsis altitude of the recovered orbit is adjusted to 30, 50, and 100 km, and -45° of AoP is given to locate sub-periapsis points near -45° of latitude on the Moon to

Table 7. Expected orbital shape of recovered orbit with periapsis altitude of 100 km

Parameters	Delta-V margin applied to RM #2 (m/s)		
	0	**100**	**200**
RM #2 Mag. (km/s)	0.207	0.307	0.407
Semi major axis (km)	4,691.369	3,375.134	2,666.888
Eccentricity	0.60399	0.452667	0.30883
Orbital period (hour)	8.041	4.896	3.436
Apoapsis altitude (km)	5,806.739	3,174.269	1,757.776
Altitude at north pole passage (km)	3,463.667	2,209.134	1,348.725
Altitude at south pole passage (km)	348.989	294.132	241.549
Altitude at ascending Node passage (km)	349.931	294.664	241.931
Altitude at descending Node passage (km)	3,458.621	2,207.635	1,348.296

*Magnitude of RM #1 is about 0.656 km/s for this case.
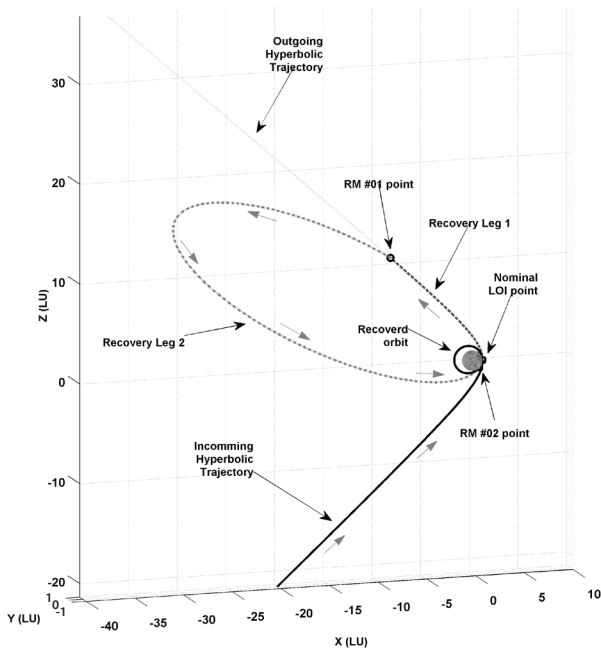
Fig. 5. Example recovery trajectory. Insertion into elliptical mission orbit with AoP -45° and 30 km of periapsis altitude.
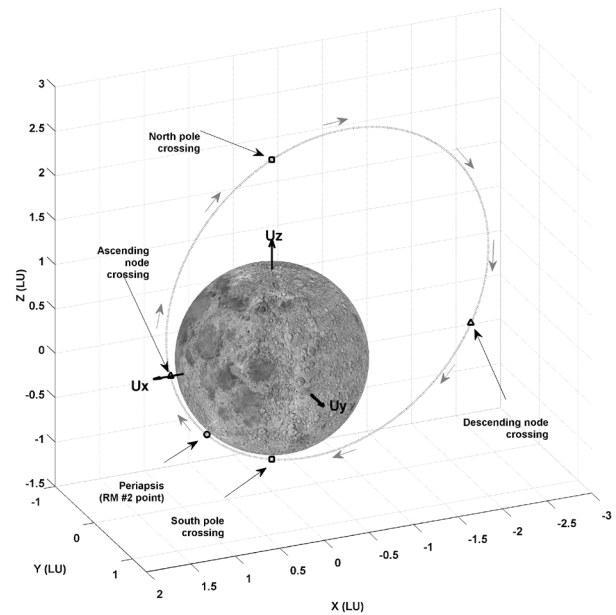
Fig. 6. Zoomed view of recovered elliptical mission orbit. Case with AoP of -45° and 30 km of periapsis altitude.

maintain low altitudes at the poles. Unlike the results shown in Table 4, the delta-V magnitude for RM #2 is limited to 0.863 km/s and also to 0.963 and 1.063 km/s to include 100 and 200 m/s of mission redundancy delta-Vs to determine their effect on the shape of the recovered mission orbit. The TOF for Leg 1 and Leg 2 shown in Tables 5-7 are selected to be 5.00 hours and 5.25 days, respectively. As shown in Tables 5-7, the altitude of the spacecraft at the lunar south-pole passage is much lower than those values in Case 1, though the north-pole passage altitude is greatly increased, which certainly is helpful to the ShadowCam operation during the south-pole passage. Another benefit from the current finding is that the spacecraft maintains an almost constant altitude from the south-pole passage to the ascending node crossings. This will help establish the payload operation plan during the flight above these regions and efforts to calibrate the collected payload data. Regarding RM #2 magnitude, the use of more delta-Vs in RM #2 lowered the overall altitude of

the recovered mission orbit, but with very trivial results. As an example, for the case when the periapsis altitude is given as 30 km (shown in Table 5), the lunar south-pole passage altitude is reduced to 271.473, 219.54, and 170.114 km when 0, 100, and 200 m/s of allocated system delta-V margins are additionally applied to RM #2 during the recovery. Current findings show that adjusting the periapsis altitude as low as possible with the use of every possible delta-V margin to RM # 2 may result in one candidate recovered orbit that may partially pursue the scientific mission after successful recovery. In Fig. 5, an example of such a recovery trajectory is shown for the elliptical mission orbit insertion case with AoP of -45° and 30 km of periapsis altitude. Fig. 6 is a zoomed-in view of the recovered mission orbit shown in Fig. 5. To scale the coordinates in both Figs. 5 and 6, note that a lunar unit (LU) (1 LU = 1,738.2 km) is used, and Ux, Uy, and Uz shown in Fig. 6 denote the unit vector components of the Moon-centered inertial frame.

339

5. CONCLUSIONS

The current work analyzed contingency trajectory options for the KPLO mission to prepare for the failure of the first LOI maneuver. There are two typical trajectory recovery options, direct recovery and low energy recovery options. The current work analyzed direct recovery options to focus on the early phase mission design and analysis. Preliminary analysis of the contingency trajectory design was performed and associated delta-Vs and trajectory characteristics were obtained. Within the direct recovery options, the possibilities of two different mission orbit recovery cases, insertion into a circular mission orbit or insertion into an elliptical mission orbit, were proposed. It was concluded that TOF Leg 1 should be within the boundaries of 4.0 to 6.0 hours and TOF Leg 2 from 5.0 to 5.5 days regardless of the recovered mission orbit's shape. It was clearly shown that RM #1 should be executed as soon as possible if the first LOI burn failed. It should be noted that a considerable amount of time for the execution of RM #1 is necessary in a real operation. At least several hours prior to RM #1 are required to obtain the exact knowledge of the spacecraft's orbital status as well as to plan and validate further recovery options. For the recovery option of direct insertion into circular mission orbit, the current work found that it can never be achieved within the delta-V budget (assumed to be about 1.063 km/s including 200 m/s of margins) with the current design baseline. However, regardless of extremely tight delta-V margins allocated to the KPLO mission, an alternative solution was discovered that maximized the scientific experiments of the KPLO mission within the boundaries of the current fuel budget. By adjusting the recovered mission orbit shape and orientation, it was expected that KPLO may partially pursue its scientific mission after successful recovery, though it would be limited. For example, if the sub-spacecraft point of the recovered mission orbit at periapsis passage (the RM #2 execution location) was adjusted to be near around -45 or 45° latitude on the Moon, and the periapsis altitude was lowered to maintain low altitudes at the polar region passage, then most of the scientific payloads currently planned to be aboard the KPLO could be partially utilized. By adjusting the recovered mission orbit shape and orientation, one of the candidate elliptical recovered mission orbits with the application of redundant delta-V margins for RM #2 execution, the KPLO mission can be continued. More in-depth analysis establishing contingency trajectory recovery options should be conducted for the KPLO mission. Upcoming analyses will consider low energy recovery cases to extend KPLO's contingency trajectory recovery options.

REFERENCES

Bae J, Song YJ, Kim BY, Initial dispersion analysis and midcourse trajectory correction maneuver of lunar orbiter, Proceedings of AIAA/AAS Astrodynamics Specialist Conference, Long Beach, CA, 13-16 Sep 2016.

Bate RR, Mueller DD, White JE, Fundamentals of Astrodynamics, (Dover Publications, New York, 1971), 228-271.

Battin RH, An Introduction to the Mathematics and Methods of Astrodynamics, Revised Edition. (AIAA Education Series, New York, 1999), 295-342.

Bechman M, Mission design for the Lunar Reconnaissance Orbiter, Proceedings of the 29th Annual AAS Guidance and Control Conference, Breckenridge, CO, 4-8 Feb 2007.

Brown CD, Spacecraft Mission Design, 2nd Edition, (AIAA Education Series, New York, 1998), 5-21.

Choi S, Song YJ, Bae J, Kim E, Ju G, Design and analysis of Korean lunar orbiter mission using direct transfer trajectory, J. Korean Soc. Aeronaut. Space Sci. 41, 950–958 (2013). https://doi.org/10.5139/JKSAS.2013.41.12.950

Gauss C, Theory of the motion of the heavenly bodies moving about the sun in conic sections: a translation of Gauss's "Theoria motus": With an appendix, (Little Brown and Company, Boston, 1857), 234-248.

Genova AL, Contingency trajectory design for a lunar orbit insertion maneuver failure by the LADEE spacecraft, Proceedings of the AIAA/AAS Astrodynamics Specialist Conference, San Diego, CA, 4-7 Aug 2014.

Gooding R, Procedure for the solution of Lambert's orbital boundary-value problem. Celest. Mech. Dyn. Astron. 48, 145-165 (1990).

Houghton MB, Tooley CR, Saylor Jr. RS, Mission design and operations considerations for NASA's Lunar Reconnaissance Orbiter, Proceedings in 58th International Astronautical Congress, Hyderabad, India, 24-28 Sep 2007.

Izzo D, Revisiting Lambert's problem, Celest. Mech. Dyn. Astron. 121, 1–15 (2015).

Kawakatsu Y, Yamamoto M, Kawaguchi J, Study on a lunar approach strategy tolerant of a lunar orbit injection failure. Trans. Jpn. Soc. Aeronaut. Space Sci. Space Technol. Jpn. 5, 1–7 (2007). https://doi.org/10.2322/tstj.5.1

Kim Y, Park SY, Lee E, Kim M, A deep space orbit determination software: overview and event prediction capability, J. Astron. Space Sci. 34, 139-151 (2017). https://doi.org/10.5140/JASS.2017.34.2.139

Lancaster ER, Blanchard CR, A unified form of Lambert's Theorem, NASA GSFC Technical Note, NASA-TN-D-5368 (1969).

Lee E, Kim Y, Kim M, Park SY, Development, demonstration and validation of the deep space orbit determination software using lunar prospector tracking data, J. Astron. Space Sci. 34, 213-223 (2017). https://doi.org/10.5140/JASS.2017.34.3.213

Liu L, Cao J, Liu Y, Hu S, Tang G, et al., CHANG'E-3 contingency scheme and trajectory, Adv. Space Res. 55, 1074–1084 (2015). https://doi.org/10.1016/j.asr.20104.11.025

Lozier D, Galal K, Folta D, Beckman M, Lunar prospector mission design and trajectory support, Proceedings of the AAS/GSFC International Symposium on Space Flight Dynamics, 11-15 May 1998, Greenbelt, MD, (1998), 297–312.

Song YJ, Kim BY, Evaluating high-degree-and-order gravitational harmonics and its application to the state predictions of a lunar orbiting satellite, J. Astron. Space Sci. 32, 247-256 (2015). https://doi.org/10.5140/JASS.2015.32.3.247

Song YJ, Park SY, Choi KH, Sim ES, Development of Korean preliminary lunar mission design software, J. Korean Soc. Aeronaut. Space Sci. 36, 357–367 (2008). https://doi.org/10.5139/JKSAS.2008.36.4.357

Song YJ, Woo J, Park SY, Choi KH, Sim ES, The earth moon transfer trajectory design and analysis using intermediate loop orbits, J. Astron. Space Sci. 26, 171-186 (2009). https://doi.org/10.5140/JASS.2009.26.2.171

Song YJ, Park SY, Kim HD, Lee JH, Sim ES, Trans lunar injection (TLI) maneuver design and analysis using finite thrust, J. Korean Soc. Aeronaut. Space Sci. 38, 998-1011 (2010). https://doi.org/10.5139/JKSAS.2010.38.10.998

Song YJ, Park SY, Kim HD, Lee JH, Sim ES, Analysis of Delta-V losses during lunar capture sequence using finite thrust, J. Astron, Space Sci. 28, 203-216 (2011). https://doi.org/10.5140/JASS.2011.28.3.203

Song YJ, Bae J, Kim YR, Kim BY, Uncertainty requirement analysis for the orbit, attitude, and burn performance of the 1st lunar orbit insertion maneuver, J. Astron. Space Sci. 33, 323-333 (2016a). https://doi.org/10.5140/JASS.2016.33.4.323

Song YJ, Lee D, Bae J, Kim BY, Kim Y, et al., Preliminary design of LUDOLP: the flight dynamics subsystem for the Korea pathfinder lunar orbiter mission, Proceedings of the 14th International Conference on Space Operations, Daejeon, Korea, 16-20 May 2016b.

Song YJ, Kim YR, Bae J, Kim BY, Evolution of the selenopotential model and its effects on the propagation accuracy of orbits around the moon. Math. Probl. Eng. 2017, 5493679 (2017). https://doi.org/10.1155/2017/5493679

Vallado DA, Fundamentals of astrodynamics and applications, 4th ed. (Kluwer Academic Publishers, Boston, 2013), 20-27.

Woo J, Song YJ, Park SY, Kim HD, Sim ES, An earth-moon transfer trajectory design and analysis considering spacecraft's visibility from Daejeon ground station at TLI and LOI maneuvers, J. Astron. Space Sci. 27, 195-204 (2010). https://doi.org/10.5140/JASS.2010.27.3.195